

POLYMER-BASED VOLUME HOLOGRAMS FOR A SURFACE-NORMAL 3X3 NON-BLOCKING WAVELENGTH-SELECTIVE CROSSBAR

Charles C. Zhou Joseph I and Ray T. Chen

Microelectronics Research Center
University of Texas, Austin
Austin, TX 78758

ABSTRACT

In this paper, we present a 3x3 non-blocking crossbar for network applications. This device is pivotal for the realization for a computer-to-computer interconnect network where both wavelength division multiplexing and space division multiplexing are employed to enhance the transmission bandwidth. We report the formation of a surface-normal wavelength selective non-blocking crossbar using photopolymer-based volume holograms in conjugation with graded index (GRIN) lenses. The elimination of edge-coupling significantly enhances the packaging reliability. Furthermore, such a configuration is compatible with the implementation of vertical cavity surface-emitting lasers where the characteristic of azimuthal symmetry is maintained in the waveguiding substrate. The prototype polymer-based volume hologram for a multiple-wavelength 3x3 crossbar is experimentally demonstrated at 755, 765, and 775 nm. The unique beam routing property of GRIN lens reduced nine wavelengths to three wavelengths while maintaining the required nine (3x3) individual interconnects. Realizing the fact that the wavelength-switching speed of semiconductor lasers is as fast as 1 nsec, we expect to build a fully packaged system with much less system latency.

NON-BLOCKING 3x3 CROSSBAR SWITCH

A crossbar is important for the realization of computer to computer interconnect. Non-blocking crossbar is preferred due to its intrinsic fast speed[1]. We demonstrate a surface-normal wavelength selective non-blocking crossbar based on a unique wavelength switching scheme where photopolymer-based volume holograms are employed in conjugation with graded index (GRIN) lenses. The schematic of the proposed crossbar is shown in Fig. 1. A prototype polymer-based volume hologram for multiple-wavelength 3x3 crossbar is experimentally demonstrated. The unique beam routing property of GRIN lens reduces nine wavelengths to three wavelengths while maintaining the required nine

(3x3) individual interconnects. The elimination of edge-coupling significantly enhances the packaging reliability. Furthermore, such a configuration is compatible with the implementation of vertical cavity surface-emitting lasers (VCSEL). The characteristic of azimuthal symmetry is maintained in the waveguide substrate due to the employment of substrate guided waves [2].

POLYMER-BASED VOLUME PHASE HOLOGRAM COUPLER

The phase gratings recorded in the photopolymer films were slanted, the central wavelength of the input surface-normal beam, i.e., 765 nm, was designed to be diffracted with a maximum efficiency at the Bragg angle. The wavelengths that deviate from the center wavelength will be dispersed at different substrate bouncing angles with less diffraction efficiency where discrete substrate modes are generated and zig-zagged within the substrate. The central wavelength bouncing angle θ_0 was set at 45° . For maximum diffraction efficiency at the central wavelength, the grating spacing Λ must satisfy the following relationship:

$$\theta_0 = 2\sin^{-1}\left(\frac{\lambda_0}{2n\Lambda}\right), \quad (1)$$

where λ_0 is the central wavelength n is the polymer refractive index.

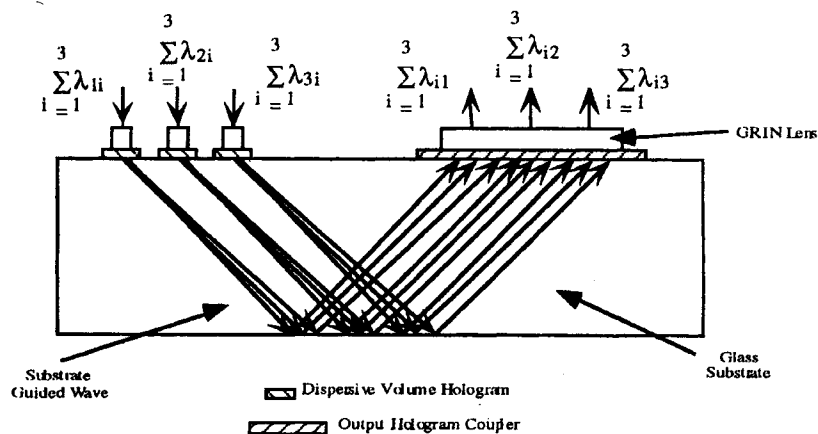


Figure 1. Polymer-based volume hologram crossbar for a surface-normal 3x3 non-blocking wavelength selective crossbar. Note that the special characteristic of the GRIN lens reduces the nine wavelengths to three, i.e. $\sum_{i=1}^3 \lambda_{i1} = \lambda_1 = 755\text{nm}$, $\sum_{i=1}^3 \lambda_{i2} = \lambda_2 = 765\text{nm}$, $\sum_{i=1}^3 \lambda_{i3} = \lambda_3 = 775\text{nm}$.

For transverse electric (TE) substrate-guided waves, the diffraction efficiency of volume hologram is[3]

$$\eta = \frac{\sin^2(v^2 + \xi^2)^{1/2}}{1 + \xi^2 / v^2}, \quad (2)$$

$$v = \frac{\pi \Delta n d}{\lambda_0 (c_r c_s)^{1/2}}, \quad (3)$$

$$\xi = -\frac{\Delta \lambda K^2 d}{8 \pi n c_s} = \frac{\Delta \theta K d \sin \Phi}{2 c_s}, \quad (4)$$

$$c_r = 1, \quad c_s = 1 - \frac{K \cos \Phi}{k_0}, \quad (5)$$

$$K = \frac{2\pi}{\Lambda}, \quad k_0 = \frac{2\pi}{\lambda_0} \quad (6)$$

$$\Phi = \frac{180^\circ - \theta_0}{2}, \quad (7)$$

where d is the hologram thickness, Δn is the refractive index modulation, $\Delta \lambda$ is wavelength difference of channel λ_1 from center wavelength λ_0 , $\Delta \theta$ is the angular dispersion corresponding to wavelength deviation $\Delta \lambda$ and θ_0 is the center wavelength bouncing angle.

CHROMATIC DISPERSION AND CHANNEL SEPARATION

From Eq. (4) we can see that change of wavelength from central wavelength results in a change of diffraction angle. The angular differences among different wavelengths were maintained as they were bounced in the substrate. A quarter pitch GRIN lens was employed to separate light beams with different wavelengths and they focused onto the output surface of a GRIN lens which functions as an output coupler connecting to a fiber array.

The angular separation due to dispersion can be derived from the Bragg condition $\cos \Phi = \frac{K}{2nk_0}$ and Eq. (4) as

$$\Delta \theta = \frac{\Delta \lambda}{\lambda_0} \tan \frac{\theta_0}{2}, \quad (8)$$

where the central wavelength was 765 nm and the bouncing angle was 45° in the experiment.

After the light beams were dispersed and bounced back to the same side of the substrate, a hologram coupler was used to couple them out at the surface normal direction. A GRIN lens was used to separate the different angular frequencies. The spot separation after GRIN lens can be predicted using paraxial ray approximation solution [4]. For a parabolic refractive index distribution of

$$n(y) = n(0) \cdot \left(1 - \frac{A^2}{2} y^2\right), \quad (9)$$

where A is the GRIN lens constant. The paraxial equation describing the ray position at a GRIN output surface is:

$$y(L) = y_0 \cos(AL) + \frac{\tan(\Delta\theta)}{A} \cdot \sin(AL), \quad (10)$$

where p is the pitch size of the GRIN lens, the $L = 2\pi p / A$ is the length of the GRIN lens. Note for a quarter pitch GRIN lens, i.e., $p=1/4$, only the second term of Eq. (10) exists; therefore, incoming beams with the same wavelength and $\Delta\theta$ came out from the same spot at the output surface of the GRIN lens. Three GRIN lenses with 1 mm diameter each were used to collimating light to the input hologram coupler. λ_{1i} and λ_{3i} ($i=1, 2, 3$) were incident 1 mm off the center of the output GRIN lens axis. On the output surface, rays with the same angle of incidence (see Fig. 1) converge to the same spot as we predicted. Therefore, employment of GRIN lenses reduces nine wavelengths to three wavelengths while keeping the required interconnectivity. The incident angle differences were provided by the dispersive volume hologram. In the configuration shown in Fig. 1, three input fibers each with a collimating GRIN lens at its end were attached surface normally to the input holographic coupler. The three wavelengths transmitted through one single fiber were dispersed into three different bouncing angles by volume hologram. As described by Eq. (10), the quarter pitch output GRIN lens separates the light beams with different colors (i.e. wavelengths). The signal beams with a same wavelength from three separate input fibers were routed to the same spot at the output surface of the quarter pitch GRIN lens, where a fiber array was attached (3 fibers in our case). Therefore by using only three wavelengths, a non-blocking 3x3 crossbar can be realized. The simulation of the three different wavelength propagation in the GRIN lens is shown in Fig. 2. The address of the sender in this case can be identified through the header encoded in the optical signal [5]. The use of GRIN lenses provides the capability of surface-normal coupling through holograms and fibers. As a result, reliable miniaturized packaging can be provided.

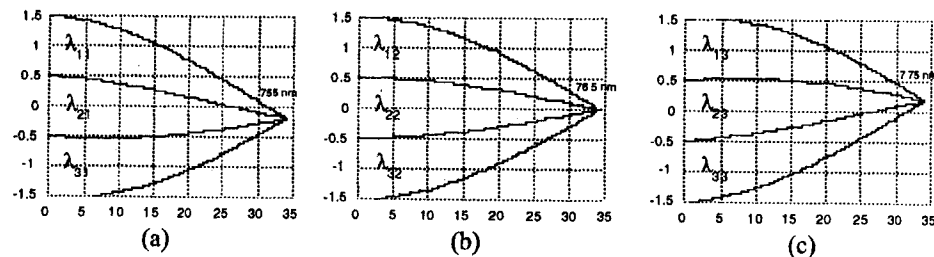


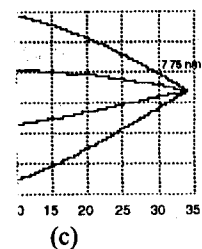
Figure 2. Ray tracing of light with different incident angles from three input angular dispersed light beams onto the quarter pitch output GRIN lens (a) $\sum_{i=1}^3 \lambda_{i1} = \lambda_1 = 755\text{nm}$ (b) $\sum_{i=1}^3 \lambda_{i2} = \lambda_2 = 765\text{nm}$, (c) $\sum_{i=1}^3 \lambda_{i3} = \lambda_3 = 775\text{nm}$.

EXPERIMENTAL RESULTS

A Ti:Sapphire tunable laser was pumped by a continuous Argon Ion laser. DuPont photo-polymer film HRF-600 having a thickness of $20 \mu\text{m}$ was employed and the hologram was recorded at 514 nm . The volume hologram was fabricated using the two-beam interference method. A microscopic objective coupled the light into a single mode fiber which had a GRIN rod lens attached at the output end. The input wavelength was monitored by an optical spectrum analyzer. The collimated light from the single mode

(10)

of the GRIN lens. of Eq. (10) exists; from the same spot diameter each were λ_{3i} ($i=1, 2, 3$) were output surface, rays not as we predicted. three wavelengths nces were provided Fig. 1, three input ce normally to the ne single fiber were s described by Eq. ith different colors hree separate input r pitch GRIN lens, y using only three lation of the three The address of the e optical signal [5]. coupling through be provided.



dispersed light beams
 $\lambda_2 = 765\text{nm}$, (c)

fiber was diffracted by the input holographic coupler and zig-zagged inside the glass substrate, and was subsequently coupled out by the output hologram coupler. The output GRIN rod lens focused the light onto different spots corresponding to different wavelength channels. A CCD camera and an eight bit frame grabber image processing system were employed to take the pictures. Spot size, channel separation and other parameters were experimentally confirmed. Fig. 3 illustrates the 3x3 interconnects. Note that λ_{11} , λ_{21} and λ_{31} are 755 nm, λ_{12} , λ_{22} and λ_{32} are 765 nm, λ_{13} , λ_{23} and λ_{33} are with 775 nm. As previously predicted, λ_{i1} , λ_{i2} and λ_{i3} ($i=1, 2, 3$) were coming out from the same spots as clearly indicated in Fig. 3. In our experiment, the average channel separation was 250 μm and average spot size less than 60 μm . The average crosstalk was less than 20 dB.

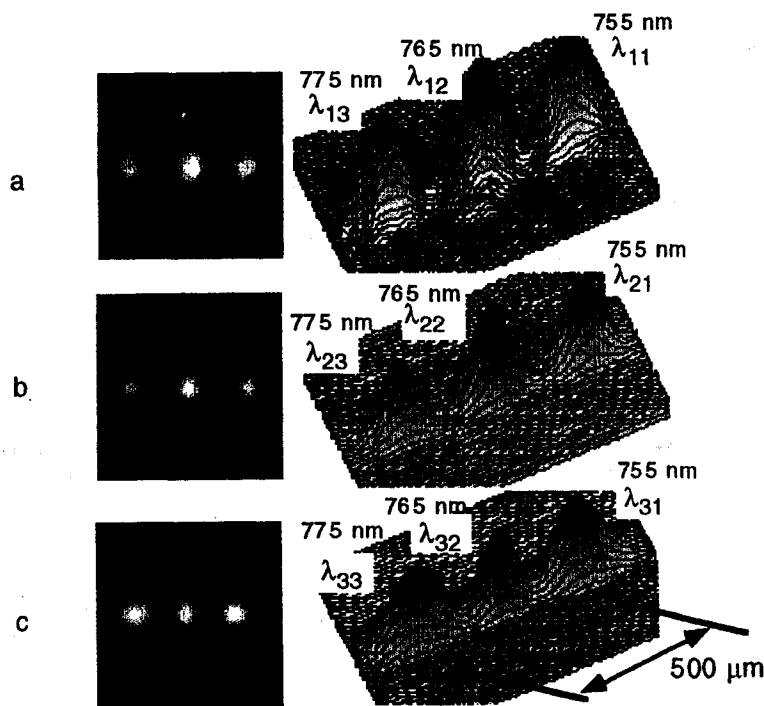


Figure 3. Images of GRIN lens output surface showing nine interconnects separation and three-dimensional intensity profile of the nine spots. (a) λ_{11} , λ_{12} and λ_{13} (b) λ_{21} , λ_{22} and λ_{23} (c) λ_{31} , λ_{32} and λ_{33} .

A summary of the results is given in Table 1. It's found that the output spectrum has the same bandwidth as that of the input. Due to the Gaussian beam nature of the substrate guided waves, the output spots are larger than the diffraction limited spots. Such an effect will be evaluated in a separate publication. The wavelength separation with the proposed configuration can be as small as 1 nm [6]. Combining our crossbar with the fast switching wavelength tunable VCSEL[7], a non-blocking 3x3 crossbar interconnects with a nano-second (10^{-9}) switching speed can be realized.

Table 1. The measurement result of three-wavelength non-blocking crossbar.

Wavelength	Spot Size (3dB)	Channel Separation
$\lambda_1 = 755 \text{ nm}$	75 μm	250 μm
$\lambda_2 = 765 \text{ nm}$	75 μm	
$\lambda_3 = 775 \text{ nm}$	75 μm	

In summary, we present the first surface-normal non-blocking crossbar based on the wavelength dispersion of a volume hologram. A 3x3 crossbar containing nine interconnections has been successfully demonstrated with wavelengths of 755, 765 and 775 nm. $\Delta\lambda$ as small as 1 nm can be implemented using the proposed architecture. The unique beam routing property of the GRIN lens employed reduces the 9 required wavelengths to 3 while maintaining the 3x3 interconnections.

ACKNOWLEDGMENTS

This research is sponsored by AFOSR, BMDO and ARPA's Center for Optoelectronics Science and Technology. The authors thank Maggie M. Li for her help.

REFERENCES

1. L. A. Bergman, A. J. Mendez and L. S. Lome, Bit parallel wavelength links for high performance computer networks, *SPIE Critical Review*, (1996).
2. M. M. Li, R. T. Chen, Sunning Tang, and Dave Gerold, Angular limitations of polymer-based waveguide holograms for 1-to-many V-shaped surface-normal optical interconnects, *Appl. Phys. Lett.* 65:1070 (1994).
3. H. Kogelnik, Coupled wave theory for thick hologram gratings, *The Bell Sys. Tech. J.* 48:2909 (1969).
4. W. M. Rosenblum, J. W. Blaker and M. G. Block, Matrix methods for the evaluation of lens systems with radial gradient-index elements, *American Journal of Optometry and Physiological Optics*, 65:661 (1988).
5. IEEE Standard for Scalable Coherent Interface (SCI), IEEE STD 1596-1992.
6. 1996 Spring quarterly Report of ARPA center for Optoelectronics Science and Technology.
7. C. Chang, J. Harbison, *et al.* Multiple wavelength tunable surface-emitting laser arrays, *IEEE J. Quan. Electr.*, 27:1368 (1991).